JOURNAL OF MATERIALS SCIENCE 28 (1993) 4940–4943

Binder distribution in Si_3N_4 ceramic green bodies studied by stray-field NMR imaging

PU SEN WANG, D. B. MINOR, SUBHAS G. MALGHAN
Ceramics Division, Materials Science and Engineering Laboratory, National Institute of Standards and Technology, Gaithersburg, MD 20899, USA

Nuclear magnetic resonance (NMR) imaging is an emerging technology which provides a unique material-diagnostic technique by *in situ* internal mapping. It can provide information not only on material distribution, but also on the chemical and physical characteristics of materials. However, due to the nuclear dipole–dipole interaction in solid state materials, NMR spectroscopic signals are normally very broad. NMR imaging based on these unresolved broad lines is extremely difficult, and resolution is poor. The binder distribution was studied in ceramic green bodies with a stray-field NMR imaging facility at a proton frequency of 163 MHz near the edge of a 9.394 T superconducting magnet. The ^1H nuclear spin echo signal from silicon nitride green bodies containing 10 wt% of either polyethylene glycol or polyvinyl alcohol as a binder was detected at 163 MHz. NMR images show a good homogeneity of the binder distribution in the cross-sections of the samples. Overall results show that the distribution of polyethylene glycol in Si_3N_4 green bodies is more homogeneous than that of polyvinyl alcohol under similar processing parameters. NMR spectroscopic results also indicate a higher moisture content in the green bodies containing a polyvinyl alcohol binder.

1. Introduction

In the manufacture of most of advanced ceramics, the starting materials are sub-micrometre sized powders. These powders possess varying degrees of chemical impurities and surface properties, depending on the synthesis process. One of the first steps in the manufacturing of ceramics is to mix these powders with polymeric surfactants in an aqueous or non-aqueous environment in order to achieve a variety of functions in the slurry and green (unsintered) ceramic. Two examples of the use of polymeric surfactants are dispersants and binders. The role of dispersants is to provide de-agglomeration and stabilization against re-agglomeration of particles as a result of steric or electrosteric interaction forces in the presence of a liquid environment. Polyacrylates of different molecular weights and composition are commonly used as dispersants for oxide and non-oxide powders where stabilization of particles is provided by the adsorption of polyacrylic ions on the negatively charged particles. This type of adsorption results in the enhancement of the net negative charge on the particles and thereby increases interparticle repulsion. Binders are added to achieve a variety of functions such as strengthening the green ceramic by binding particles, lubrication of particles to promote interparticle sliding, and plasticizing to improve the flexibility of binder films. Some of the binders used in ceramic powder processing are polyvinyl alcohol, polyethylene glycol, cellulose and dextrin.

With such a large number of organic chemicals present in the slurries of ceramic powders, these chemicals interact. The complexity of the bulk and interface interactions of powder, water, inorganic impurities, and organic surfactants are not well-understood. These interactions lead to inhomogeneities in the suspensions and green body in the form of agglomerates, a non-homogeneous distribution of surfactants, voids and chemical segregation. These inhomogeneities, once formed in the green state, remain in the final ceramic; thus they form defects in the sintered ceramic. These defects are considered to be the main cause of the problems associated with the repeatability of manufacturing processes.

In advanced ceramic components, the failures often occur due to defects such as voids and large-scale chemical segregations undetectable by conventional methods. Nuclear magnetic resonance (NMR) imaging is an emerging technology which provides a unique material-diagnostic technique by *in situ*, internal mapping. It can provide information not only on the material distribution (nuclear spin density), but also on the chemical and physical characteristics of these materials (nuclear spin relaxation times). In a ceramic green body, the binder distribution is a critical parameter that affects the final ceramic's mechanical, thermal and electrical properties, and its reliability. An understanding of the interfacial reactions between the binder and ceramic powders under various processing parameters is essential to alleviate binder

0022–2461

distribution related problems in ceramic processing technology. Efforts have been made to improve this understanding [1–8].

Since it was first publicized in 1973 [9], much effort has been spent in developing NMR imaging for medical, biological, and materials applications. Considerable advancements have been accomplished in the medical and biological applications because the samples involved are in a mobile state. However, due to the nuclear-dipolar broadening in solids, the development of NMR imaging for application to solid materials has been difficult.

The spatial resolution, δ, in NMR imaging can be related to the spectroscopic linewidth, v, and the magnetic-field gradient, G, by the following equation:

$$\delta = v/\sigma G$$

where σ is the gyromagnetic ratio of the nucleus observed. In solids, especially hard solids like ceramics, the linewidth due to the nuclear-dipolar interaction is often a few thousand times larger than in mobile samples because of the restriction in atomic motion. Consequently, line narrowing and large field gradients are the two factors critical to a successful NMR imaging technique for solids.

Considerable efforts have been made to develop various techniques for the improvement of line narrowing in NMR spectroscopy [10–11]. These techniques are readily applied to imaging so that a better resolved solid image can be achieved. They range from the development of a multiple-pulse sequence to multiple quantum coherence [12–20]. However, line broadening still remains as an obstacle to NMR spectroscopy in solids. Thus a large magnetic-field gradient is required to offset line broadening for a useful resolution in NMR imaging. To develop a large field-gradient from gradient coils is not an easy task. The design of the hardware and software often depends on the nature of the experiment. To generate a large field-gradient to compensate for a wide-line NMR signal for image construction is also very challenging [21, 22]. This paper reports the results of organic binder distribution in a ceramic green body by NMR imaging utilizing a large field gradient provided by a stray field together with a series of solid echoes for nuclear detection [17].

2. Experimental procedure*

The following materials were used to prepare the samples: Polyacrylic acid (PAA), 5000 MW, Aldrich. Polyethylene glycol (PEG), 1000 MW, Aldrich. Polyvinyl alcohol (PVA) 13000–23000 MW, Aldrich. Si_3N_4, UBE SN-E-10, (median size 0.2 μm, specific area, 10 $m^2 g^{-1}$, Ube Industries); and HNO_3, reagent grade, 1.024 N.

* Certain commercial equipment, instruments, or materials are identified in this paper in order to specify the experimental procedure adequately. Such identification does not imply recommendation or endorsement by the National Institute of Standards and Technology, nor does it imply that the materials or equipment identified are necessarily the best available for the purpose.

Silicon nitride was added to distilled water and the slurry was acidified with HNO_3 to a pH of 5.8–6.0, and mixed with prediluted binders. The slurry was subjected to ultrasonic vibration with a 1.9 cm diameter probe at 270 W for 1 min and then allowed to stand for 1 min. This procedure was repeated three times for each slurry. During the ultrasonic treatment, the slurries were kept cool by an ice–water bath. The slurry was transferred to a polyethylene tube (75 mm long, 15 mm outer diameter, 12 mm inner diameter) with a Teflon bottom stopper and centrifuged at 2700 r.p.m. (revs per minute) for 30 min. The supernatant liquid was withdrawn by a pipette and the cast sample was heated in a vacuum oven at 40 °C overnight at 5% relative humidity. The resulting solid samples were stored in a desiccator and used for NMR studies.

A cylindrical sample of 12 mm diameter and 10 mm thickness was glued by epoxy to a sample holder (a ring with an inner diameter slightly larger than 12 mm). The sample and the holder were attached to an extension rod from the first rotation ring at the joint of a "screw driver" for the second rotation. Since stray-field imaging is a new technique, its principle will be explained in Section 3. The sample moisture content was analysed by a Bruker MSL-400 spectrometer at 400.13 MHz.

3. Results and discussion

3.1. Principle and operation of the stray-field NMR imaging facility

The stray-field NMR imaging facility was assembled around a Bruker MSL-400 wide-bore spectrometer. This unique NMR imaging facility for the study of solids utilizes the large gradient in the stray field. A planar surface under the edge of the superconducting coil in a 9.394 T magnet system is used for this purpose. At this surface, a static field-gradient strength of approximately 80 T m^{-1} was found [23–24]. The resonance frequency for protons at this surface is approximately 163 MHz instead of 400 MHz. Since the field is static in nature, the sample must be moved to obtain spatial information.

The resonant-probe head consists of moving parts for linear motion of the sample and the resonant coil and for rotations of the sample. In this manner, a three-dimensional projection can be made. A spherical resonant coil of 18 mm diameter was built around the sample and the holder. The coil was designed so that half of it can be easily removed from the probe for sample loading and unloading. When the sample is moved up through the surface of a large gradient along the z-axis of the magnet (parallel to the gradient direction), a maximum of 512 points will be irradiated by a solid-echo multipulse train to detect the nuclear-echo signal [17]. This linear movement can be repeated as many times (number of scans) as desired and echo signals can be accumulated to achieve a good signal-to-noise ratio. When this one-dimensional mapping is complete, the sample rotates in the yz-plane and then continues scanning for its nuclear echo signals. After the sample completes a 360° rotation in

the *yz*-plane, a two-dimensional map can be constructed by back projection of these echo signals. To construct a three-dimensional picture, the sample must be rotated away from the *yz*-plane. All these movements are controlled automatically by an ASPECT 3000 computer.

The precise three-dimensional motion (one linear and two rotational dimensions) was controlled by a motion-control unit which was connected to a second modulator which was initially designed for cross polarization in the spectrometer. This control unit drives three step-motors in the gear box which is connected to the moving part of the resonant probe. Meanwhile, the control unit continuously monitors the precise position and motion of the sample optically.

Since resonance was observed not at the centre but at the edge of the magnetic field, the resonant coil was designed to observe 163 MHz instead of 400 MHz, the magnetic strength at this sensitive surface is only approximately 3.828 T instead of 9.394 T. The displacement distance for each step of the step-motor driving the linear motion is 37.5 μm. This gives a maximum resolution of 37.5 μm in a picture irradiated by 512 points. However, the experiment currently only irradiates every other point, and so the current resolution is no better than 75 μm.

A solid-echo train of $(\pi/2)_x - \tau - (\pi/2)_y - 2\tau -$ echo $- (\pi/2)_y - 2\tau -$ echo... was used to produce a nuclear-echo signal in solids. Typically, a train of eight pulses is used. The $\pi/2$ pulse width is 4 μs for our spectrometer at the proton frequency (163.7 MHz).

3.2. Binder distribution in the silicon nitride ceramic green bodies

Fig. 1 shows an example of a cross-sectional view of the PEG distribution in a green body containing 10 wt % binder. White regions have high binder concentrations. A fairly homogeneous distribution of the binder was observed for this sample in this direction. Note that the brightest area, at the top of this picture, is not due to the binder. It is a signal from the epoxy used to glue the sample to the holder: epoxy contains protons. The spectrum on this picture is an intensity profile of the binder distribution along the vertical arrow. This arrow can be changed to any angle so a more quantitative expression of spin density can be obtained. Pictures taken perpendicular to this surface indicate that there is a low-binder zone in this sample. Fig. 2 gives an example. The dark area in the center represents a region which contains a low concentration

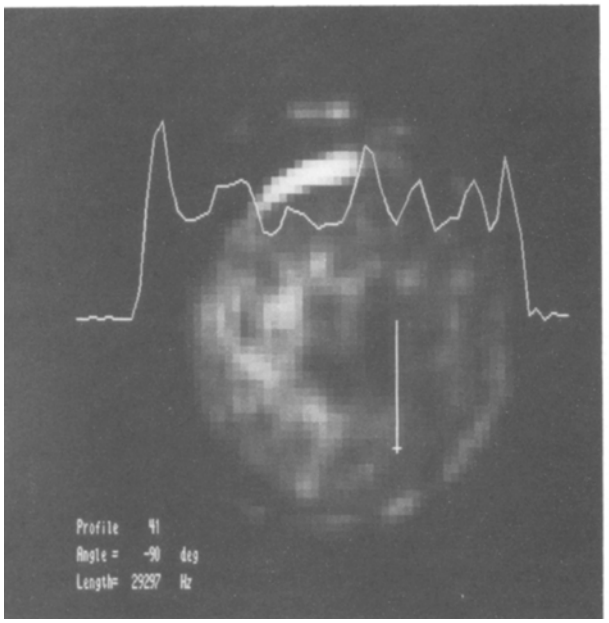

Figure 1 A cross-sectional view of the binder distribution in a 10 wt % PEG in a silicon nitride green body obtained by stray-field NMR imaging. Angle $-90°$, length 29297 Hz.

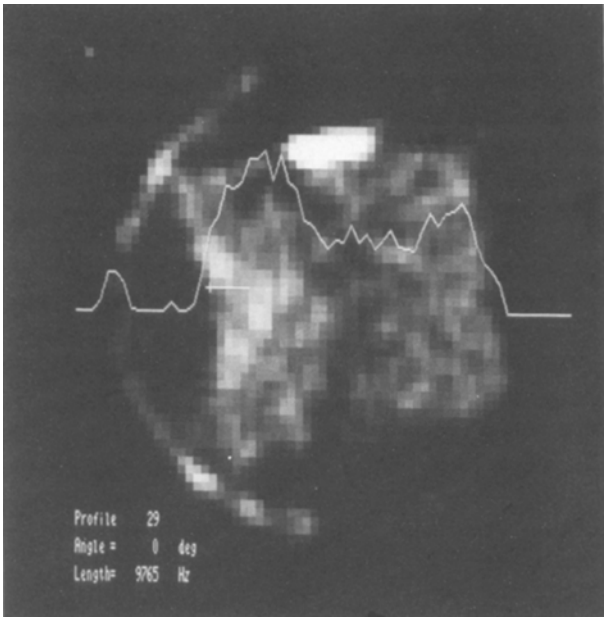

Figure 2 A vertical view of the binder distribution in a 10 wt % PEG in a silicon nitride green body obtained by stray-field NMR imaging. Angle 0°, length 9765 Hz.

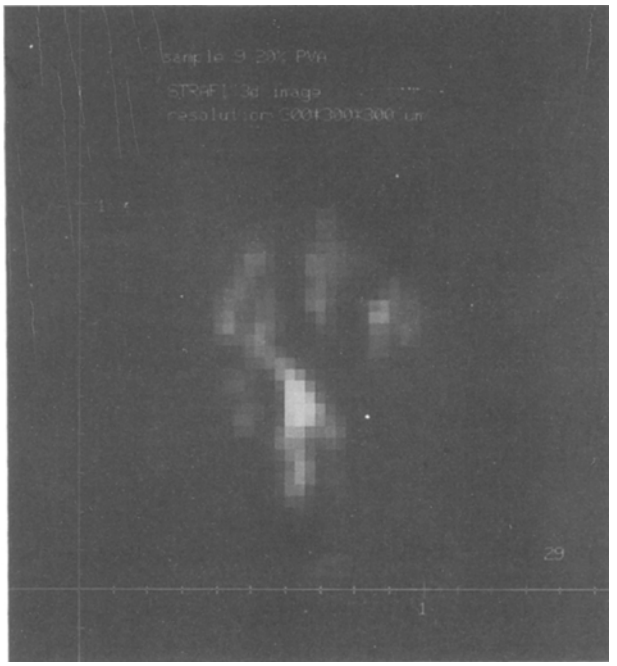

Figure 3 A cross-sectional view of the binder distribution in a 10 wt % PVA in a silicon nitride green body obtained by stray-field NMR imaging.

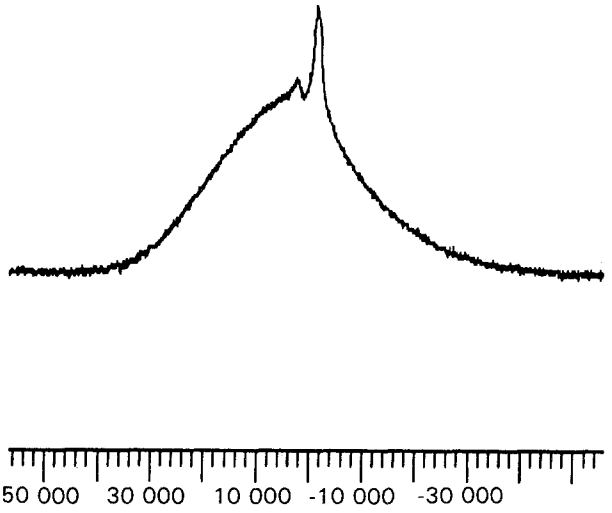

Figure 4 400.13 MHz proton FT–NMR spectrum of a silicon nitride green body containing 10 wt % PVA as a binder.

of binder. It can be easily seen that the left of the picture has a higher binder concentration than the right. A spectroscopic profile made horizontally across this picture proves this distribution. A calculation of the proton intensity from this spectroscopic profile shows that along the region of the horizontal arrow the PEG-binder concentrations in the right-hand and central areas are only 68% and 47%, respectively, of the left-hand area. In addition, both mapping and spectroscopic profile detect some weak proton-containing material on the left-hand side of the radio-frequency resonant probe. This may be due to the lacquer coated on the wire used to build the probe.

Fig. 3 gives an example of the PVA distribution in a cross-sectional view of a silicon-nitride green body containing 10 wt % binder and 100 p.p.m. of dispersant. Once again there is a fairly homogeneous binder distribution along this direction. The overall results indicate that the distribution of PEG in Si_3N_4 green bodies obtained by centrifugal casting is more homogeneous than in those containing PVA processed under similar conditions. A spectroscopic ^1H FT–NMR study at 400.13 MHz for these samples suggests that the green bodies containing PVA have a higher moisture content. Fig. 4 represents a proton FT–NMR spectrum at 400.13 MHz of a sample containing 10 wt % PVA (the same sample was used in Fig. 3). The broad signal is due to the solid protons in the PVA which have a strong dipole–dipole interaction. The narrow peak is the result of moisture in the sample.

4. Conclusion

A plane of large field gradient (80 T m^{-1}) in the stray field near the edge of the superconducting coil was utilized in a high-resolution solid NMR imaging facility at a proton frequency of 163.7 MHz. Nuclear-echo signals were detected by a multiple radio-frequency pulse sequence. A resolution of 75 μm was achieved by this equipment. Silicon nitride green bodies prepared by centrifugal casting with PEG or PVA as a binder were examined for homogeneity in three dimensions. Generally, samples containing both binders exhibited uniform distribution in a given cross-section. However, the distribution of PEG was more homogeneous than that of the PVA in a Si_3N_4 green body prepared under similar conditions. ^1H FT–NMR at 400.13 MHz indicated that the sample containing PVA had high moisture content. This moisture is thought to be that retained in agglomerates formed as a result of using PVA binder.

Acknowledgement

This project is partially supported by the Office of Intelligent Processing of Materials, National Institute of Standards and Technology. The technical assistance from Drs K. Zick and D. G. Cory of Bruker Instrument is also appreciated.

References

1. J. L. ACKERMAN, W. A. ELLINGSON, J. A. KOUTCHER and B. R. ROSEN, "Nondestructive characterization of materials II" (Plenum Press, New York, 1987) p. 129.
2. W. A. ELLINGSON, J. L. ACKERMAN, L. GARRIDO, J. D. WEYLAND and R. A. DIMILLIA, *Ceram. Engng. Sci. Proc.* **8** (1987) 503.
3. L. GARRIDO, J. L. ACKERMAN, W. A. ELLINGSON and J. D. WEYLAND, *Ceram. Engng. Sci. Proc.* **9** (1988) 1465.
4. J. L. ACKERMAN, L. GARRIDO, W. A. ELLINGSON and J. D. WEYLAND, "Nondestructive testing of high-performance ceramics" (American Chemistry Society, Washington, DC, 1988) p. 88.
5. K. HAYASHI, K. KAWASHIMA, K. KOSE and T. INOUYE, *J. Phys. D* **21** (1988) 1037.
6. W. A. ELLINGSON, P. S. WONG, S. L. DIECKMAN and J. L. ACKERMAN, *Amer. Ceram. Soc. Bull.* **68** (1989) 1180.
7. W. A. ELLINGSON, P. S. WONG, S. L. DIECKMAN, J. P. POLLINGER, H. YEH and M. W. VANNIER, *Ceram. Engng. Sci. Proc.* **10** (1989) 1022.
8. L. GARRIDO, J. L. ACKERMAN and W. A. ELLINGSON, *J. Magn. Reson.* **88** (1990) 340.
9. P. C. LAUTERBUR, *Nature* **242** (1973) 190.
10. M. MEHRING, "High resolution NMR in solids" (Springer-Verlag, Berlin, 1983).
11. U. HAEBERLEN, "High resolution NMR in solids: Selective averaging", Advances in Magnetic Resonance Supplement 1, (Academic Press, New York, 1976).
12. J. S. WAUGH, L. M. HUBER and U. HAEBERLEN, *Phys. Rev. Lett.* **20** (1968) 180.
13. P. MANSFIELD, *J. Phys. C* **4** (1971) 1444.
14. P. MANSFIELD, M. J. ORCHARD, D. C. STALKER and K. H. B. RICHARDS, *Phys. Rev. B* **7** (1973) 90.
15. W. K. RHIM, D. D. ELLEMAN and R. W. VAUGHAN, *J. Chem. Phys.* **58** (1973) 1772.
16. J. G. POWLES and P. MANSFIELD, *Phys. Lett.* **2** (1962) 58.
17. J. H. STRANGE, *Phil. Trans. Roy. Soc. Lond. A* **333** (1990) 427.
18. D. G. CORY, A. N. GARROWAY and J. B. MILLER, *J. Magn. Reson.* **87** (1990) 202.
19. A. N. GARROWAY, J. BAUM, M. G. MUNOWITZ and A. PINES, *J. Magn. Reson.* **60** (1984) 337.
20. D. G. CORY, "Solid state NMR imaging", Annual Reports on NMR Spectroscopy (Academic Press, New York) **24** (1992) 88.
21. D. S. WEBSTER and K. H. MARSDEN, *Rev. Sci. Instr.* **45** (1974) 1232.
22. P. MANSFIELD and B. CHAPMAN, *J. Magn. Reson.* **72** (1987) 211.
23. A. A. SAMOILENKO and K. ZICK, *Bruker Report* **1** (1990) 40.
24. A. A. SAMOILENKO, D. YU ARTEMOV and L. A. SIBEL'DINA, *Russ. J. Phys. Chem. (UK)* **61** (1987) 1623.

Received 24 September
and accepted 21 October 1992